# Chapter 17
# Rock-Avalanche Size and Runout – Implications for Landslide Dams

T.R. Davies and M.J. McSaveney

## 1 Introduction

### 1.1 Factors Affecting Landslide-Dam Stability

A common and widespread hazard associated with landslides is river damming. If the dam fails, it releases impounded water as a potentially destructive dambreak flood, which sweeps the debris of the dam and any accumulated reservoir sediment to the river downstream, causing severe aggradation and progressive channel instability. Landslide-dam stability depends to a large extent on the dam size relative to the flow of the river it blocks, and on the dam material. These in turn depend on the nature of the triggering event, the source material and on processes that modify the material in its travel. The rock fragmentation that occurs during rock-avalanche motion results in a distinctive grading in the interior of a deposit, while the surface and upper few metres of the deposit is much coarser, less intensely comminuted rock. Landslide dams formed by blockslides are composed of relatively large, intact blocks of material; the fragmentation that influences the motion of the block is confined to a thin basal layer. Such dams are less likely to fail than those formed by rock avalanches.

### 1.2 Landslide Size

The impact of a landslide on society is determined by many factors but principally its location, speed, and size. Location is with reference to position in the landscape, and in relation to people and their infrastructure; it is not a fundamental landslide property. Size and speed convey information relating to a landslide's impact on its surroundings. They are useful information to know in advance of a landslide's

T.R. Davies (✉)
Department of Geological Sciences, University of Canterbury, Christchurch, New Zealand
e-mail: tim.davies@canterbury.ac.nz

occurrence. Landslide size can mean any of the quantities of mass, volume, and area that indicate how big it is, or might be, before and after failure. For landslide dams, volume is a crucial factor; can this be determined in advance of occurrence?

In 1991, the summit and northern flank of New Zealand's highest peak fell in a huge rock avalanche. What determined the size of this, or any other historical landslide? Why was it not larger (or smaller)? Mt Cook has had previous rock avalanches and the shape of this and other peaks derives from episodic gravitational release of rock masses. What is the statistical distribution of such landslide sizes? Are rock avalanches larger end-members of a rockfall probability-density distribution, or are rockfalls and rock avalanches fundamentally different? Mount Cook is episodically shaken in great earthquakes, but not in historical time. What is the likely release volume at Mount Cook in the next great earthquake? This event has a probability of 10% in the next 20 years!

In March 1929, a $M_L$ 6.9 earthquake triggered a release of $55 \times 10^6$ m$^3$ from Falling Mountain, on the main divide of New Zealand's Southern Alps. What determined this volume, and not some other? If the earthquake had been larger, would more have fallen? Why is the volume of this rock avalanche such an anomaly in the region's rockfalls and landslides of March 1929? We cannot yet answer any of these "size" questions, but we wish to address whether such questions have answers.

## *1.3 Effects of Dynamic Grain Fragmentation*

In recent papers [3, 4] we proposed that the remarkably long travel distance of large rock avalanches results from internal dispersive stresses caused by dynamic grain fragmentation during runout. We also suggested that grain fragmentation at the base of large low-angle blockslides explains their extraordinarily long travel [4]. Knowing the mechanical modifications that occur in rock avalanches and blockslides is critical in determining the amount of motion and in assessing landslide-dam stability; this paper summarizes our understanding. We then consider how the presence of finely fragmented rock affects dam stability.

## 2 Regional Landslide Hazard Assessment

## *2.1 Probabilistic Landslide Hazard Analysis – A New Zealand Example*

What is the volume of the largest landslide that might be expected in the Kyrgyz Republic in an average year? This is a most readily answered type of "size" question. It can be answered only through probabilistic analysis of Kyrgyz landslide data. Unless a site has a long record of repeating landslides, such landslide data are likely to be for a large area, and will not be site specific. If we had this Kyrgyz data, we could estimate from it the probability of a landslide of a particular volume

occurring within the susceptible area of the Kyrgyz Republic, but we would not be able to predict precisely where or when it might occur.

The New Zealand large landslide inventory (www.geonet.org.nz) records location and area for all known large landslides in New Zealand, but few ages are known. The New Zealand landslide catalogue has fewer data, and less precise locations, but it records time of occurrence. For North Island, the inventory contains data on 5,773 landslides. Analysis provides information on relative sizes of landslides, but nothing on rate of occurrence.

Systematic data collection for the catalogue started in August 1996. It records landslides as they occur, compiled by daily monitoring of news media and other sources, and special mapping for events that trigger many landslides. The catalogue is "complete" for landslides with footprint areas $>10,000$ m$^3$, and provides useful data on landslide rate despite the short (7 year) record.

North Island landslide-area probability-density distributions can be modelled as either inverse-gamma [13] or double Pareto [24] distributions (Fig. 17.1); the larger-area portion is fractal, with a fractal dimension of $2.56 \pm 0.05$ [6]. Catalogue data have statistically the same fractal dimension, and combining the two analyses allows exceedence probabilities of given landslide areas over time to be estimated (Fig. 17.2) [6].
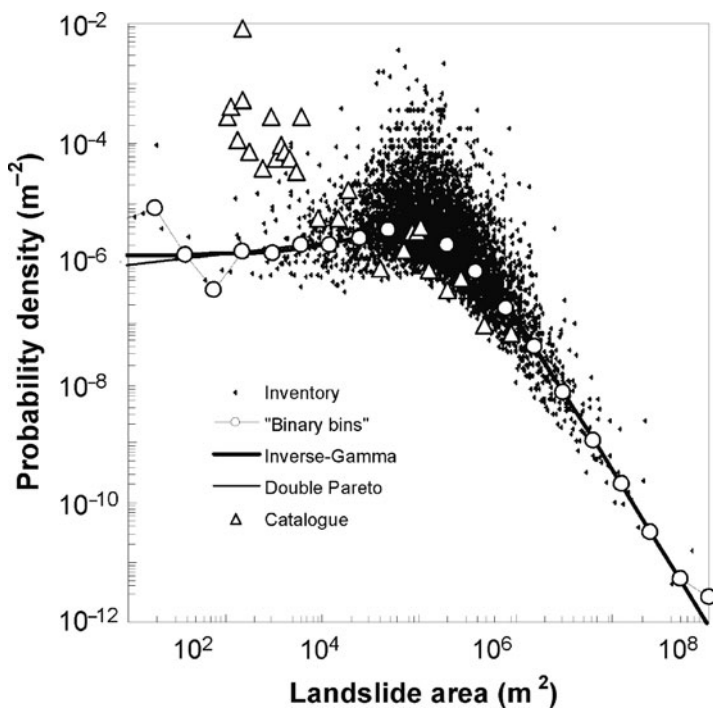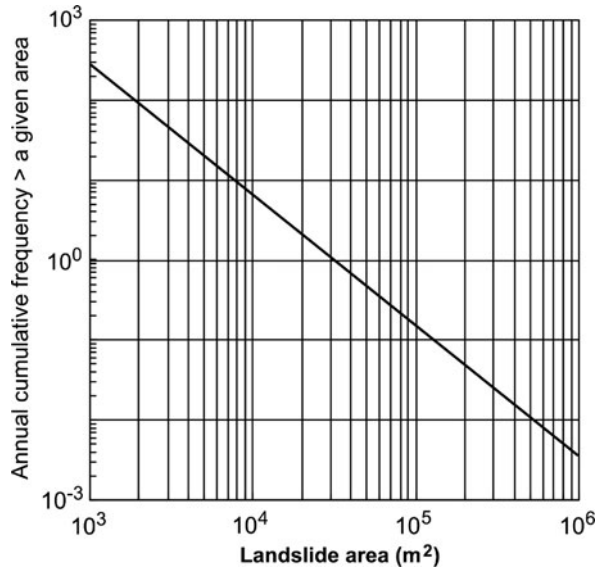


**Fig. 17.1** Probability-density distributions of landslide areas for North Island in the New Zealand large landslide inventory (5,773 landslides) and landslide catalogue (53 landslides) [6]

**Fig. 17.2** Probabilistic
landslide analysis for North
Island landslides answers the
question of what sizes of
landslides might be expected
over some specified interval
(1 year) [6]



Probabilistic landslide hazard evaluation is achievable with appropriate data.
There are no methodological barriers in estimating the size of landslide expected
in a given area over a specified interval; the only barrier is the chronic paucity of
data.

## 3 Endogenic ("Self-Induced") New Zealand Rock Avalanches

### 3.1 Background

Many rock avalanches in New Zealand's Southern Alps fall without recognized triggers, or prior warning. One at Mt Cook (Fig. 17.3) [14], two at Mt Fletcher [14], and one at Mt Adams [10] appear to be induced by static gravitational stress in the mountain rock mass. Seismic records indicate that the bulk of the energy from the release at Mt Cook in December 1991 dissipated in 2 min [14, 17] (Fig. 17.4 top). Witnesses describe the main release as over in 15 min, but the roar of falling rocks continued for an hour and a half, and tremor from falling rocks was recorded for most of the day.

Rockfalls also began at Mt Fletcher in December 1991, and continued sporadically until the ridge north of Mt Fletcher fell in rock avalanches in May and September 1992. On May 2, witnesses watched several large rockfalls during the day, and a large piece of the slope fell that night. Seismic records indicate that the bulk of the energy in May dissipated in 3 min, and similarly in September, but with different phasing and lesser amplitude (Fig. 17.4 centre). There had been numerous

**Fig. 17.3** The east face of Mount Cook collapsed in December 1991 releasing an avalanche of $12 \times 10^6$ m$^3$ of rock and ice. Based on seismogram (Fig. 17.4) interpretation, the bulk of the rock mass broke from the source in the first 20 s of the rapidly escalating collapse, and almost all of the mass was in simultaneous motion. Photo by Lloyd Homer

**Fig. 17.4** Vertical component seismograms of four large rock avalanches in New Zealand's Southern Alps showing evidence of different phasing of mass release in the various rock avalanches [17]. All from the one station (Berwen) and displayed at equal gain
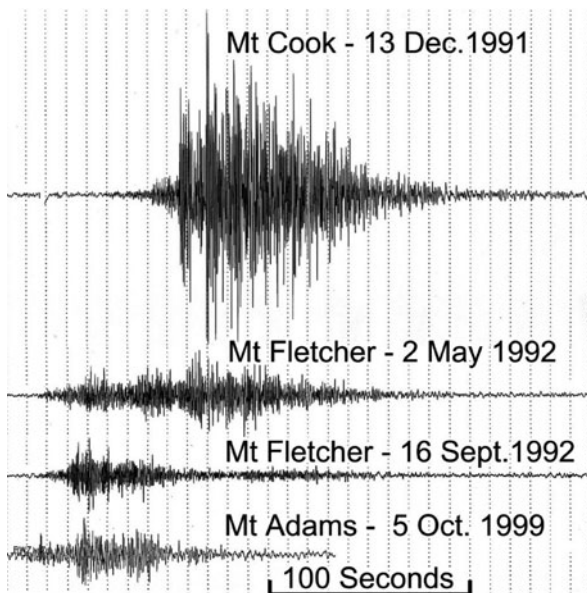
rockfalls from Mt Fletcher over at least the last 50 years, with some of them being many thousands of cubic metres in volume, such that the ablation area of Maud Glacier has been kept covered by rock debris. On 6 October 1999, a rock avalanche of some 10–13 × $10^6$ $m^3$ fell from near the summit of Mt Adams and blocked Poerua River [10]. It was a more abrupt seismic event than the other three examples (Fig. 17.4 lower) indicating one dominant release, as at Mt Cook.

## 3.2 Development of Release Volumes

To model a deep-enough release surface at Mt Cook, McSaveney [14] invoked rock-mass inhomogeniety – a stress-release joint system subparallel to the face of the mountain, but dipping slightly more steeply. Because of the low factor of safety calculated for small failures near the base of a buttress, he suggested that the avalanche did not instantaneously release on one surface, but was a rapid cascade of releases that extended up the slope. This analysis is too simplistic. The seismic record comes from the highest rate of energy dissipation in a cataclysmic phase of failure. Preceding this was an unrecorded phase of accelerating creep. Stress redistribution during creep is likely to have progressively developed a single release surface. If creep began at the most highly stressed location, it would have begun near the surface in the lower slopes of a rock buttress, and propagated from there up and into the slope, intersecting numerous stress-release joints. Creep did not lead to any external change that could be recognized as unusual by untrained observers scaling the summit in the early hours of the previous day, or in passing aircraft during the latter parts of the day until sunset. Accelerating creep in the lower slope is likely to have shown as an increasing frequency of rockfalls, but no frequency change was reported. We surmise that the accelerating creep phase was brief, possibly less than a few hours. No unusual rockfall or ice-avalanche activity was noted until people were alerted by the main collapse. Retrogressive failure appears to have been "minor" and due to stress-release cracking in the remaining "intact" rock mass. An "interrupted" slump of ~0.5 × $10^6$ $m^3$ remains on the right upper flank of the release surface to this day. Spalling of rocks from the release surface continued for some weeks, diminishing exponentially from a maximum in the moments after the primary release. Hence, we reason that a cataclysmic release of the rock avalanche took away a 700-m buttress and the summit in one flowing surge of rapidly collapsing rubble on a single release surface. The principal release volume (~90% or more) was in the main event, followed by an exponentially declining series of stress-release rockfalls that diminished in volume and frequency over weeks.

The Mt Fletcher release sequence differed from that at Mt Cook. First, the Mt Fletcher releases were not isolated events. There had been sporadic rockfalls and rock avalanches over decades, with two causally related avalanches within months. Second, the seismic records of the three rock avalanches are different (Fig. 17.4). If Mt Cook was a single-phased release, then the two Mt Fletcher events cannot be single phased. The May and September rock avalanches fell from the same location and travelled the same path; seismogram differences can only be from

differing styles of release of the source masses. The May seismograms have been read [17] as indicating that the May event escalated "slowly" and had one main but "extended" phase. The September release escalated more rapidly but was not as large as in May. As the first phase in September began to die away, a late, smaller release phase began, and was prolonged relative to the first. The releases from Mt Fletcher may be retrogressive failures. The whole sequence of rockfalls and rock avalanches can be interpreted as a series of retrogressive failures. The underlying cause of the sequence appears to be rock-mass creep consequent on melting of ice formerly buttressing a structurally weak rock mass on the right lateral margin of Maud Glacier [14]. The structural weakness arises because Mt Fletcher is formed in the hanging wall of the low-angle, reverse Main Divide fault, and its rock mass is very closely jointed. Stress redistribution within Mt Fletcher is likely to have been over the long term during the thinning of Maud Glacier over more than 100 years. The creep phase has been ongoing for decades, during which, the rock mass has dilated. A protracted phase of accelerating creep on the lower slopes of the ridge led to an increasing rockfall frequency. There were several large falls in the hours before the rock avalanche in May 1992. Diminishing stress-release spalling of rocks from the failure-surface scar continued for months after both major rock avalanches. The principal mass of the release sequence was split between two main events in a ratio of 2.6:1, with perhaps as little as 10% in pre- and post-rock-avalanche rockfalls [17].

## *3.3 Prospects for Prediction*

In the above failure scenarios, the initial Mt Cook rock-avalanche mass was created by propagation of a release surface during creep prior to cataclysmic failure. Hence static 3-D stability analysis of the slope, with appropriate generalized rock-strength parameters would have given a useful estimate of the release volume. The summit flanks of Mount Cook appear to have a modal release volume of ~3.6–36 × $10^6$ m$^3$ under static loading. The location and volume of the next endogenic failure is determined by the current topography and generalized in situ rock-mass strength and might be found by searching the existing topography for the site causing the highest local stress concentrations in the rock mass. A great earthquake on the nearby Alpine fault could trigger some of these impending "self-induced" failures, but also could trigger a much-more deeply seated failure (see Sect. 4). In the Mt Fletcher scenario, the rock avalanches are only parts of a lengthy sequence of progressive failure. Static 3-D stability analysis of the slope with appropriate generalized rock-strength parameters can be expected to give only an estimate of the total volume, and not of the individual components. Nevertheless, we infer that the flanks of Mt Fletcher have a gross modal failure volume similar to that at Mt Cook, ~3.6–36 × $10^6$ m$^3$ under static loading. To determine the volume of the next failure in the sequence will require specific knowledge of the thickness and extent of the dilated, creeping rock mass of the larger failure. The obvious rockfall hazard of the site precludes any prospect of obtaining in situ geotechnical parameters for the mountainside.

# 4 Earthquake-Triggered Rock Avalanches and Rockfalls

## 4.1 New Zealand's 1929 Falling Mountain Rock Avalanche

On 6 March 1929, a landslide of $55 \times 10^6$ m$^3$ of closely jointed rock was released from Falling Mountain (Fig. 17.5) [16]. Although it is the only historical rock avalanche from this location, it was not the first release from the local valley wall. An adjacent valley was truncated prehistorically at Tarn Col by cataclysmic loss of its headwaters [16].

At the top of the source area, the main scarp is about 900 m wide. The main scarp and flanking scarps of the release surface bite deeply into the mountainside. The slide was thicker (up to 100 m) in the crown area. There are no visible crown cracks.

## 4.2 Controls on Volume

The remnants of Falling Mountain show evidence of "ridge renting" or sackung, and it is tempting to attribute the size of the failure to the spacing of specific defects associated with the ancient sackungen. However, there are many mountainsides in the
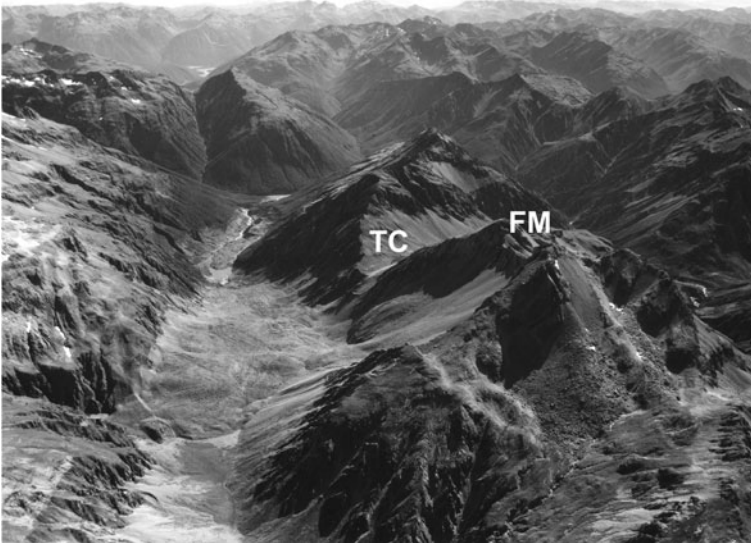


**Fig. 17.5** Falling Mountain (FM) on the main divide of New Zealand's Southern Alps. The distinctive deep release surface indicates an earthquake trigger. The release volume is almost as predictable as the earthquake location and magnitude. Location of the truncated valley at Tarn Col (TC) is indicated. A sackung ridge crosses the *right* mid-flank of the mountain. Photo by Lloyd Homer

vicinity with similar sackungen and no rock avalanches, and Sackungen still survive on Falling Mountain. The geometry of surviving defects does not suggest that the landslide release surface was controlled by pre-existing defects; rather, favourably located defects were exploited. Major defects remain. Small rockfalls occurred from surrounding slopes in the area, but no other long-runout landslides occurred in that event. The Falling Mountain rock-avalanche volume is an extreme outlier among landslides triggered by the March 1929 earthquake. The controls on the volume appear to have been the precise location and magnitude of the triggering earthquake. We suggest that the now-destroyed mountain mass resonated at a frequency that was strongly represented in the earthquake shaking, and shook itself apart during the earthquake.

## 4.3 Prospects for Prediction

There is prospect for a specific estimate of earthquake-triggered landslide volume when earthquake location and magnitude are predictable. Meanwhile, there are other challenges for seismic slope stability.

There is a family of deep, cirque-like, earthquake-induced rock-avalanche scars that differ markedly from the "thin-slab" failures that occur between earthquakes. These deep-seated failures arise because the rock mass under seismic loading behaves as if it were a weak rock under static loading. It is not in fact weak; failure arises because the triggering force is large in comparison to the rock-mass strength. Typically, the rock strength is exceeded by a large amount. Important factors in seismic triggering of landslides are local resonance and topographic amplification of wave energy, including double-amplitude displacements at reflection of waves. These are not only surface phenomena, they also occur at internal rock-mass defects and velocity contrasts.

A question arises in earthquake-induced landsliding: "If the earthquake were larger, or closer, would the landslide have been larger?" This question cannot be answered empirically: it is impossible to test the same slope to failure under different loading conditions. Among our colleagues who claim that landslide size is determined by pre-existing defects, are some who claim that a larger or closer earthquake would have triggered a larger landslide. How is this possible if pre-existing defects are the control? Do the defects move? An explanation of the role of rock-mass defects comes from failure theory. When materials break, they always break at pre-existing defects, but the breakage is not defect controlled – other, sometimes-weaker defects do not break. As stress increases in the rock mass, pre-existing defects that are appropriately aligned to the stress tensor grow, while others are inhibited. Failure occurs when sufficient defects coalesce. In this model of failure, a larger or closer earthquake causes a larger landslide from the same site if it activates different and deeper defects. The mechanism of seismic triggering of landslides in brittle rock, however, is not well understood and a number of plausible hypotheses are available. This limits the practicality of numerical modelling to accurately determine the volume of failure. One method of overcoming the inability to investigate

the question empirically is through physical modelling. We currently are developing apparatus to investigate this problem.

## 4.4 Rockfalls from New Zealand's 2003 Fiordland Earthquake

The New Zealand landslide catalogue includes 457 landslides that were triggered by a $M_W$ 7.2 shallow earthquake in Fiordland on August 21, 2003 [20]. Volumes of these landslides were visually assessed during several flights over the area, and most volumes are expressed as a range (e.g. 250,000–500,000 m³) or as maxima (e.g. <1,000 m³) or minima (e.g. >100,000 m³), which present some difficulty in numerical analysis. To overcome the difficulty, values were arbitrarily assigned to the indeterminate volumes according to a few simple rules. Initial inspection of the data suggested a fractal distribution of rockfall volumes, and so indeterminate volumes were randomly distributed within their assessed range according to the fractal distribution of the population. Volumes assessed as <1,000 m³ were assumed to lie within the range 10–1,000 m³, and those assessed as >100,000 m³ were given a range of 100,000–125,000 m³. To ensure that any particular randomly selected volume under these rules did not bias the analysis, the procedure was repeated 5 times, and the 5 values for each landslide were averaged. The entire process was iterated until there was no significant change in the power-law exponent (slope of the distribution in log-log space), indicating that the indeterminate volumes were distributed within their ranges in the same distribution as the total. The probability density distribution of rockfall volumes >100 m³ from the August 2003 Fiordland earthquake appears to be fractal over the entire range of assessed volumes, with a power-law exponent of $-1.5 \pm 0.3$ (Fig. 17.6a).
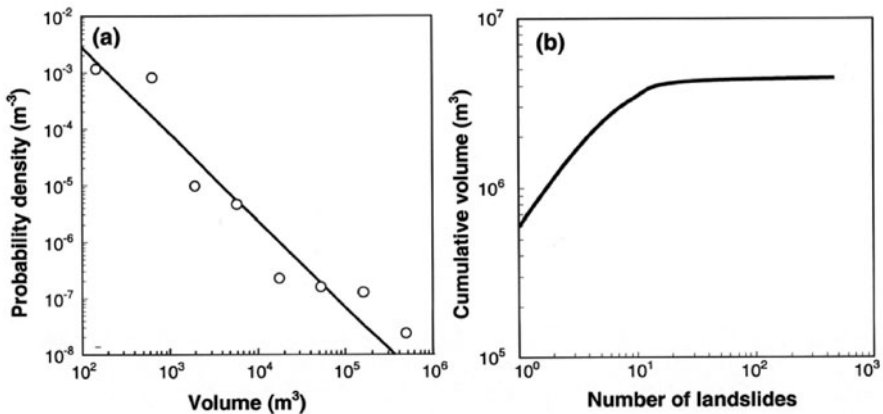


**Fig. 17.6** (**a**) Probability density distribution of rockfall volumes in the August 2003 Fiordland NZ $M_L$ 7.1 earthquake. Line represents a power law with an exponent of $-1.5$. (**b**) Cumulative rockfall volume in the Fiordland earthquake showing that most of the volume is in the few largest rockfalls

The cumulative rockfall volume (Fig. 17.6b) is very revealing of the prospects for prediction of the total volume of landslides in a given earthquake. The largest 1% of the Fiordland rockfalls contains 52% of the total rockfall volume, and the largest 10% contains 96%. The few large landslides that contributed most of the volume are likely to have had specific and unusual reasons for being so large, and so they were not amenable to useful statistical prediction. In the 1929 Arthur's Pass earthquake that gave rise to the $55 \times 10^6$ m$^3$ Falling Mountain rock avalanche, the total volume of landslides is likely to be only a little more than the volume of that one landslide, and we have already discussed the difficulties in predicting the size of this landslide prior to the earthquake.

## 5  Summary – Landslide Size

A long-recognized fundamental landslide problem is predicting the reach for hazard assessment. Let us consider in a flight of fancy that we have solved the problem of the physics of landslide runout and have an infallible numerical model for predicting landslide reach. We can be certain that a key input parameter in the model will be information on the landslide mass or volume. We have to know how big a landslide will be in order to predict its potential runout, or the size of the dam it may form. There are people (probably many people) among us who do not believe that the size of landslides can be determined in advance without a great deal of costly geotechnical investigation. Is it possible that they are mistaken? There is an analogue computer out there that gets the answer right every time. If more effort is put into researching this "big" problem will we obtain useful answers in the intermediate or longer time? One starting point might be to identify failure mechanisms where there might be "simple" solutions, and those where there might not. When we know how big a landslide is going to be, then the calculation of its shape at the end of its runout will have much more meaning.

Edifice shape appears to be much more important than specific, weakest defects in determining the shapes of release surfaces, and so the probability-density distribution of potential failure sizes from a site is intrinsically estimable from topography, general knowledge of the rock-mass characteristics, and the probability-density distributions of potential triggering events. When a landslide will occur is quite another question.

## 6  Stresses Within a Fragmenting Rock Avalanche

### 6.1  Grain Bridges, Elastic Limits and Super Stress

Of particular importance in the flow of granular materials is the presence within the shearing grain mass of "bridges" (or arches), which are filamentous assemblages of grains aligned in the direction of maximum compressive strain of the mass (at 45° to
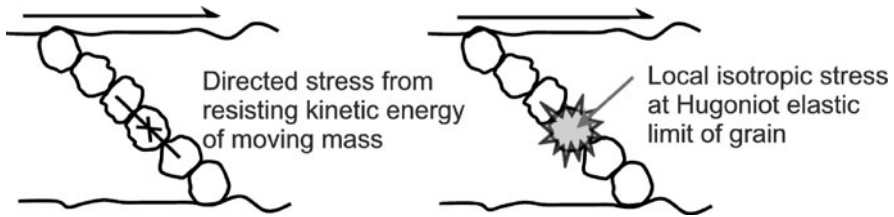
**Fig. 17.7** Idealized sketch of a grain bridge where confining pressure inhibits slip and rotation of grains and the weakest grain in the bridge fails by fragmentation, creating a local dispersive pressure of at least the Hugoniot elastic limit of the grain material

the flow direction; Fig. 17.7). Such bridges are a well-recognized hazard in industrial grain flows [19]; they also have been observed in experimentally deformed fault gouge [21]. Shear strain forces grains against adjacent grains, and stresses are transmitted between grains across bridges of grains in compressional contact. Shear ceases if the grain bridges do not fail. They mostly fail by slip between adjacent grains, and by rolling of grains, and these processes control the rate of grain-mass deformation.

A less frequent grain-bridge-failure mechanism is grain breakage: when stresses within a bridge are sufficiently high, the weakest grain can break. A characteristic of breaking brittle rock is a delay between stress application and rupture while micro-cracks form and propagate [22, 23]. When the stress in a grain bridge exceeds the strength, or elastic limit of the weakest grain, a degree of "super-stressing" is inevitable and the grain explosively disintegrates into fragments – a process we term "fragmentation". In the explosion, an isotropic dispersive force is transferred to all adjacent grains, and while fragmentation is taking place, the shear resistance within the volume occupied by the fragmenting grain is vanishingly small or zero.

## *6.2 Magnitude of Stresses*

A one-dimensional numerical model [12] has been used [3] to show that the time- and depth-averaged internal longitudinal dispersive stress needed to simulate the runout of two rock avalanches in New Zealand is of the order of five times the average geostatic stress of the deposit; in the case of the $55 \times 10^6$ m$^3$ Falling Mountain event [3] this is about 2.5 MPa. If the stress generated by a single fragmenting grain were 2.5 MPa, then every grain in the avalanche would need to fragment simultaneously to develop the required stress, and the isotropic dispersive stress at all points within the translating debris mass would exceed the geostatic stress by about a factor of five. This would cause the whole mass to explode in every direction at about 5 g (J.N. Hutchinson, Imperial College, London, *pers. comm.* 2003). There is no field evidence for such behaviour. It therefore cannot be the case that all (or even the majority) of grains are fragmenting simultaneously, so the local stress due to a grain fragmenting must be much greater than the spatially averaged dispersive stress.

With a small proportion of grains fragmenting at any time, the upward vertical component of the dispersion caused by any particular fragmentation event is fully reversed by gravity before the next event occurs in the vicinity. No net work is accomplished in the vertical direction by this mechanism. Hence local, intermittent high isotropic dispersive forces do not necessarily cause general upward motion of a granular mass. By contrast, instantaneous longitudinal dispersions are not reversed by gravity, but persist until the next fragmentation event in the vicinity. The absence of general upward explosion of rock avalanches thus is not evidence for the absence of locally high isotropic dispersive stresses during runout.

Experimental evidence of the magnitude of the dispersive stress generated by rock failure comes from early inelastic unconfined compression tests on a variety of rock types at low shear rates ($10^{-5}$ s$^{-1}$) [25]. Two modes of failure are reported; one (Type I) in which failure envelopes showed decreasing stress with increasing strain, and one (Type II) in which axial strain briefly reversed against the applied compressive stress. In the latter case, if the failure stress path follows the envelope during rapid stress application, the dispersive stress generated by failure exceeds the applied compressive stress. Such Type II behaviour, once initiated, requires no further input of energy to complete the fragmentation, and failure proceeds rapidly and explosively; this occurs often in dynamic grain fragmentation [15]. Because Type I behaviour does not result in a reversal of strain at failure, we make the conservative assumption that the local dispersive stress generated by a fragmenting rock particle is approximately equal to the unconfined compressive strength of the particle.

In the Falling Mountain example, the local fragmentation-induced dispersive stress is of the order of 0.5 GPa [4]; to obtain a spatially averaged stress of 2.5 MPa then requires that one grain in about 200 is fragmenting at any instant.

### 6.3 Direction of Stresses

Fragmentation of a rock particle in the shear field of a large rock avalanche delivers non-isotropic forces to its surrounding grains if it breaks into only a few pieces. However, most break into many pieces, and the number of fragmentation events occurring in any sizable aggregate of grains is large enough that the integrated effect of even non-isotropic individual stresses will be that of a uniformly isotropic stress. In addition, only isotropic stresses – not shear stresses – can be transmitted in materials stressed above their Hugoniot elastic limits. The ubiquitous presence of finely comminuted rock shows that rock-avalanche materials have been repeatedly stressed beyond their elastic limits.

### 6.4 Grain-Size Distribution of Rock Avalanche Material

Grain-size distributions of rock avalanches and fault gouges from published and unpublished data from New Zealand and elsewhere (Fig. 17.8) all have a fractal dimension close to 2.58, a value corresponding to a three-dimensional geometry
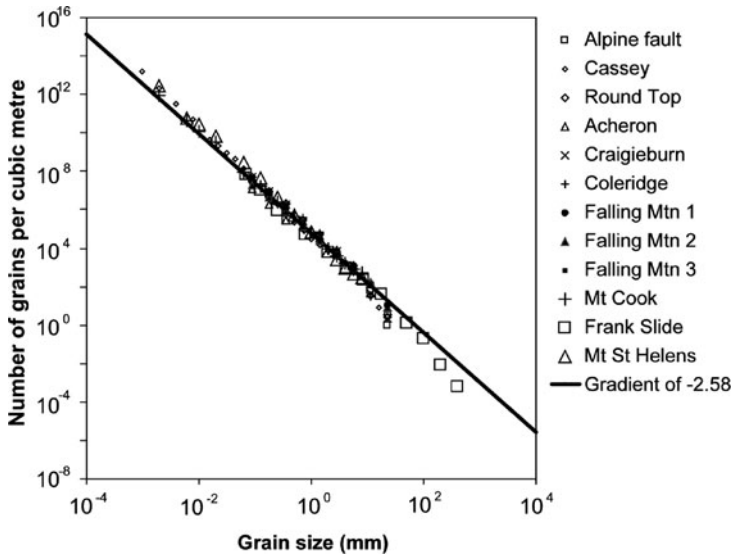
**Fig. 17.8** Rock avalanche grain-size distributions (Alpine fault and Cassey are fault gouges). Frequency is expressed as number of grain per m$^3$ assuming spherical grains of density 2,650 kg m$^{-3}$

that equalises and minimises the probability of fracture of all particles. Thus all grains present in a rock avalanche are equally likely to fragment at any given time.

## 6.5 Fragmentation Occurs Throughout the Runout

It is fundamental to our explanation that fragmentation occurs throughout the runout, and we have much supporting evidence:

- shattered undisaggregated clasts are often found close to the distal margin at depth within rock-avalanche deposits. Such clasts could not have been shattered at the onset of motion and retained their close proximity and arrangement for the duration of the avalanche.
- the deposit of the Vaiont landslide, which travelled only a relatively short distance before halting, is not fragmented [8].
- the Köfels landslide deposit is not completely fragmented; in particular, one component of the mass that was halted by an obstruction is fairly intact [8]

The reason for fragmenting lies in strain-induced fracture of grains during grain-bridge failure, and it must continue so long as shear deformation continues. Dispersive stresses due to fragmentation are therefore present throughout rock-avalanche fall and runout.

## 7  Conceptual Model of Fragmentation

Our concept of rock-avalanche fragmentation (Fig. 17.9) is that particles of all sizes are fragmenting at any one time, each generating a local isotropic dispersive pressure, the integrated longitudinal component of which causes increased spreading during translation. In the Falling Mountain rock avalanche, the local dispersive stress generated with each fragmentation is assumed to be ~0.5 GPa. The grain-size distribution (and therefore the fractal dimension) does not vary with depth below the carapace [7], suggesting that the spatial probability of occurrence of fragmentation events is the same at all levels below the carapace.
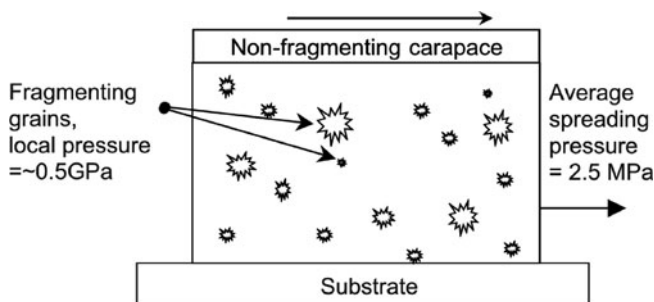


**Fig. 17.9** Diagram of fragmentation in rock avalanches. Fragmentation of individual grains is represented by stars of various sizes; particles of all sizes are fragmenting at any one time, each generating a high local isotropic dispersive pressure, the integrated longitudinal component of which causes increased spreading during translation. Pressures refer to those in the Falling Mountain rock avalanche discussed in Sect. 4.1

## 8  Laboratory Confirmation

We have designed and built a shallow cone-and-plate rheometer for measuring the direct and shear stresses developed in shearing granular rock material that is under sufficient direct stress that shearing is accompanied by fragmentation (Fig. 17.10). Briefly, the stationary roof is loaded with the chosen direct stress. The sample container is rotated about its axis at a chosen rate; the geometry ensures that the shear rate is uniform across the width and depth of the sample. The sample is sheared and, due to the high direct stress, grains fragment. A load cell attached to the torque-measuring annulus records the shear stress transferred from the rotating base to the roof. The apparatus and its ancillaries are described in greater detail elsewhere [2].

At low shear rates (~10 s$^{-1}$) similar to those found in rock avalanches, with a maximum grain diameter less than 20% of the shearing material depth, shearing of fragmenting granular materials (coal, argillite and limestone) gave a ratio of shear to direct stress (or friction coefficient) that was always similar to that of the same material when not fragmenting.
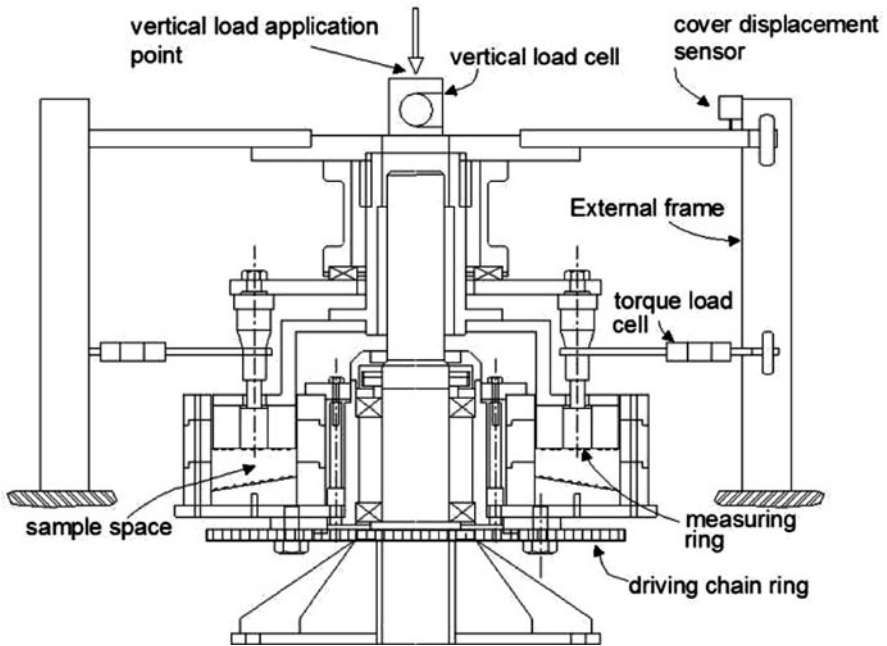
**Fig. 17.10** Principle of fragmenting rheometer in which test data (Fig. 17.11) were measured
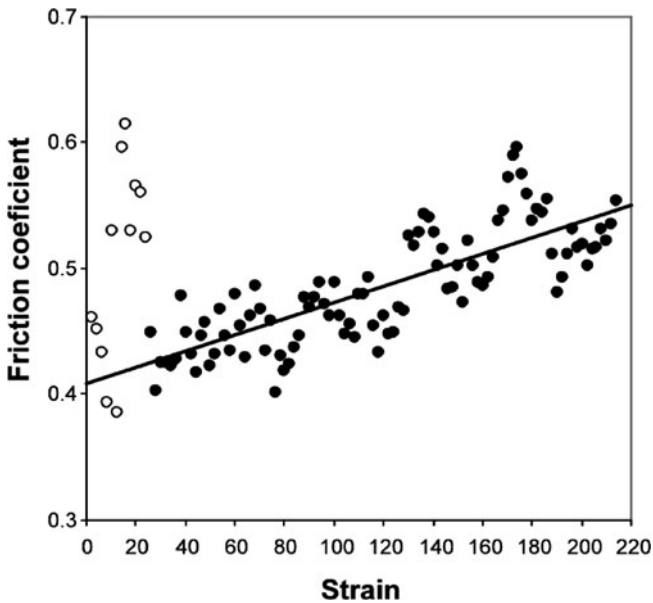


**Fig. 17.11** Sample test data for fragmenting coal. Shear rate is ~100 s$^{-1}$, overburden is 300 kPa. Trend line (slope 0.00065 $\pm$ 0.00005/unit of strain) is fitted to data of filled circles. Maximum reduction in friction coefficient is 20%

However, when we loaded the shear cell with large particles (up to the same size as the shear cell depth) and subjected them to greater shear rates (~100 s$^{-1}$), the measured friction coefficient was significantly lower than that for non-fragmenting shearing material. This was because the large fragmenting grains exerted a dispersive direct stress on the upper and lower cell boundaries, reducing the effective direct stress on the remaining non-fragmenting grains and thus reducing the frictional force they could apply to the torque-measuring annulus. Typical test data (Fig. 17.11) show that the friction coefficient increased with shear strain, as grain sizes in the cell reduced through fragmentation, reducing the ability of fragmenting particles to deliver direct stress simultaneously to both upper and lower cell boundaries. The reduction in friction coefficient allows the reduction in effective direct stress to be calculated, which is the value of the stress generated by fragmenting grains; thus the fragmentation stress is measured by this experiment. For coal grains, the fragmentation-generated stress was about 0.15 MPa, of the order of 1% of the unconfined compressive strength of the coal, indicting that about 1 grain in 100 was fragmenting at any time.

## 9  Application to Blockslides

A remarkable prehistoric landslide deposit at Waikaremoana, North Island, New Zealand is interpreted as a low-angle rapid blockslide [1, 5], in which a 1.2 km$^3$ intact block of sandstone moved about 2 km on a sandstone surface sloping at about 6–8° to the horizontal at a speed of up to 30–50 ms$^{-1}$ (Fig. 17.12). The long, accelerating travel on a very low-angle surface requires that there was very low frictional



**Fig. 17.12**  Waikaremoana blockslide and landslide-dammed Lake Waikaremoana. Photo by Lloyd Homer

resistance to motion of the block on the sandstone substrate. We suggest that this low friction was due to fragmentation at the sliding interface, given the inevitable initial rugosity expected of any failure surface within intact rock [5].

A 0.3 m thick layer of finely ground rock at the base of the displaced block recently has been proven by drilling (R. Beetham, GNS, Lower Hutt, N.Z. personal communication), and is interpreted as the fragmented material. The vertical dispersive pressure generated by fragmentation of individual clasts, if applied directly to the underside of the detached intact block, provides sufficient vertical force to support most of the weight of the block during motion (Fig. 17.13). This reduces the normal stress between the block and its substrate, and hence the frictional resistance to motion; a fragmenting rock at the substrate-block interface cannot transmit any shear force because it is stressed above its Hugoniot elastic limit. Analysis of the stresses involved shows that fragmentation of one particle in about 35 is required [5] to explain the acceleration of the block to the inferred velocity [1, 5].
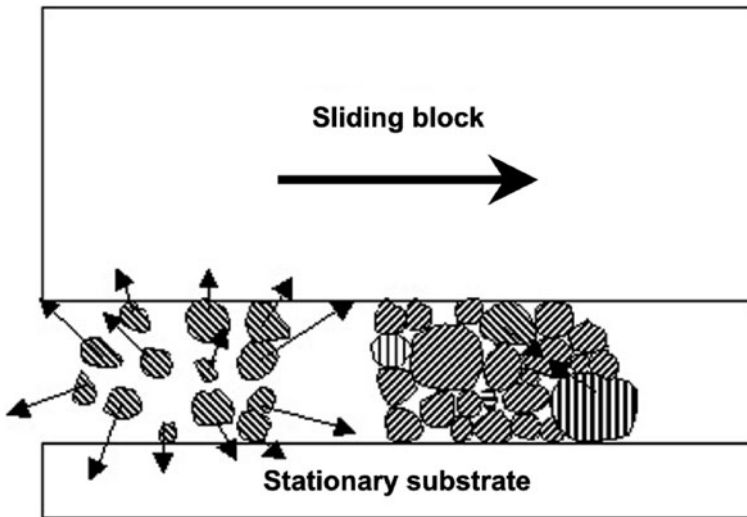


**Fig. 17.13** Fragmenting grain supports weight of block reducing direct stress on adjacent shearing non-fragmenting debris

## 10 Application to Landslide Dams

Fragmented rock-avalanche debris dominates the material properties of landslide dams, and the dams' ability to resist failure due to overtopping, slope failure or piping. A large rock-avalanche deposit is a relatively unstructured mass of all grain sizes, apart from the top several metres, which has a higher proportion of larger clasts. The surface layer of large clasts often gives rock-avalanche deposits an appearance of being comprised completely of angular boulders (Fig. 17.14).

**Fig. 17.14** Mystery Creek (Green River) rock-avalanche deposit, British Columbia, Canada showing uniformly large surface clasts forming a carapace on the rock avalanche. The carapace is formed by collapse of the rock mass along joints. Its mass is its only contribution to the dynamics of the rock-avalanche runout process. Note figure, trees and power pylons for scale

However, the material beneath the boulder carapace is finely fragmented (Fig. 17.15), and matrix – rather than clast-supported. If the carapace is disrupted by water flow, the interior is highly erodible. The finer subsurface material, however, is likely to be of low permeability due to its wide grading and consequent very small average void size. It is therefore likely that seepage rates will be low following emplacement of the dam. Slumping of the downstream dam face due to daylighting of the phreatic surface is likely to require a long time to occur, making this mode of failure relatively unlikely prior to overtopping. This was the case with the Poerua landslide dam in Westland, New Zealand [10, 11]. Piping failure also has a lower likelihood than overtopping, because the widely graded material of the dam acts as an efficient filter. Even when seepage has developed it is unlikely that void spaces will be sufficiently large to allow particle migration.

Not all overtopping events cause failure; the Poerua dam initially overtopped about 2 days after emplacement, but did not fail until 5 days later, in a higher flow event [11]. This could be due to saturation of the downstream slope by seepage from the overflow water, or to translation of the phreatic surface to the downstream face during the interval.

Alternatively, the failure could have been caused simply by the greater and more erosive flow. Some landslide dams do not fail. Recent attempts to identify the factors that determine whether or not a landslide dam will fail [9, 18] conclude that dam-material size is a dominant factor in determining the long-term stability of the dam. Landslide dams caused by blockslides (e.g. Waikaremoana) usually comprise intact bedrock with a few large fractures but no general disaggregation into fines. Seepage through a blockslide dam is often much greater than through a rock avalanche dam,

**Fig. 17.15** Section through Mystery Creek (Green River) rock-avalanche deposit, showing the finely crushed interior. Dynamic grain fragmentation in the failure of grain bridges is the cause of the comminution. Grain fragmentation imparts a dispersive stress of the magnitude of the Hugoniot elastic limit of the rock material appropriate for the local strain rate and confining stress

and the probability of failure is much lower. The Waikaremoana dam is now the site of a hydropower development. Prior to this development, the seepage through the debris was large, discharging all the lake inflow except in major storms.

## 11  Conclusions

- Edifice shape appears to be more important than specific, weakest defects in determining release-surface shapes, and so the probability-density distribution of potential failure sizes from a site is intrinsically estimable from topography, general knowledge of the rock-mass characteristics, and the probability-density distributions of potential triggering events.
- The dispersive stress generated by fragmenting rock particles is equal to or greater than the rock's Hugoniot elastic limit under the prevailing conditions. In order to explain the runout of the Falling Mountain rock avalanche, about one particle in >~200 would need to be fragmenting at any time.
- Fragmentation takes place throughout the runout phase of rock avalanches.
- The grain-size distribution of rock-avalanche debris has a fractal dimension corresponding to a particle arrangement that equalises and minimises the probability of fragmentation of each individual particle.
- Low-angle rapid blockslides result from low frictional resistance to block motion, caused by intense fragmentation under the block generating forces sufficient to support most of the block weight.

- The stability of a landslide dam is related to the grain-size distribution within it. The relative rarity of landslide dam failures due to seepage, slumping or piping can be explained wide grain-size distribution and very small average void size of the dam material.
- Landslide dams formed by blockslides are less likely to fail than those formed of fragmented debris. Seepage through substantial cracks in the block is likely to prevent significant overtopping.

# References

1. Beetham, R.D., McSaveney, M.J. and Read, S.A.L. (2002) Four extremely large landslides in New Zealand, in J.Rybar, J. Stemberk and P. Wagner (eds.), *Landslides*. A.A. Balkema, Rotterdam, pp. 97–102.
2. Davies, T.R., Deganutti, A.M. and McSaveney, M.J. (2003) A high-stress rheometer for fragmenting rock, in L. Picarelli (ed.) *Proceedings of the International Conference on Fast Slope Movements: Prediction and Prevention for Risk Mitigation*. Naples, May 11–13, 2003 Vol. 1, pp. 139–141.
3. Davies, T.R.H. and McSaveney, M.J. (2002) Dynamic simulation of the motion of fragmenting rock avalanches, *Canadian Geotechnical Journal* **39**, 789–798.
4. Davies, T.R.H. and McSaveney, M.J. (2003) Runout of rock avalanches and volcanic debris avalanches, in L. Picarelli (ed.) *Proceedings of the International Conference on Fast Slope Movements: Prediction and Prevention for Risk Mitigation*. Naples, May 11–13, 2003 Vol. 2.
5. Davies, T.R., McSaveney, M.J. and Beetham, R.D. (2006) Rapid block glides: slide-surface fragmentation in New Zealand's Waikaremoana landslide, *Quarterly journal of Engineering Geology and Hydrogeology* **39**, 115–129.
6. Dellow, G., McSaveney, M.J., Stirling, M.W., Lukovic, B., Heron, D.W., Berryman, K.R. and Peng, B. (2004) Probabilistic landslide hazard in North Island, New Zealand, from landslide magnitude-frequency distributions, Unpublished file report. Institute of Geological & Nuclear Sciences Ltd, Lower Hutt, New Zealand.
7. Dunning, S.A. (2004) Rock avalanches in high mountains – A sedimentological approach, Unpublished PhD Thesis University of Luton, UK.
8. Erismann, T.H. and Abele, G. (1999) *Dynamics of Rockfalls and Rockslides*. Springer, Heidelberg, 316p.
9. Ermini, L. and Casagli, N. (2003) Prediction of the behaviour of landslide dams using a geomorphological dimensionless index, *Earth Surface Processes and Landforms* **28**, 31–47.
10. Hancox, G.T., McSaveney, M.J., Davies, T.R.H. and Hodgson, K.A. (1999) Mt Adams rock avalanche of 6 October 1999 and the subsequent formation and breaching of a large landslide dam in Poerua river, Westland, New Zealand, *Institute of Geological and Nuclear Sciences Science Report* **99/19**, 33p.
11. Hancox, G.T., McSaveney, M.J., Manville, V.R. and Davies, T.R. (2005) The October 1999 Mt. Adams rock avalanche and subsequent landslide dam-break flood and effects in Poera River, Westland, New Zealand, *New Zealand Journal of Geology and Geophysics* **48**, 683–705.
12. Hungr, O. (1995) A model for the runout analysis of rapid flow slides, debris flows, and avalanches, *Canadian Geotechnical Journal* **32**, 610–623.

13. Malamud, B.D., Turcotte, D.L., Guzzetti, F. and Reichenbach, P. (2004) Landslide inventories and their statistical properties, *Earth Surface Processes and Landforms* **29**, 687–711.

14. McSaveney, M.J. (2002) Recent rockfalls and rock avalanches in Mount Cook National Park, New Zealand. in S.G. Evans, and J.V. DeGraff (eds.). *Catastrophic landslides: Occurrence, mechanisms and mobility*. Geological Society of America Reviews in Engineering Geology, **15**, 35–70.

15. McSaveney, M.J. and Davies, T.R.H. (2006) Rapid rock-mass flow with dynamic fragmentation:inferences from the morphology and internal structure of rockslides and rock avalanches, in S.G. Evans, G. Scarascia-Mugnozza, A. Strom and R. Hermanns (eds.), *Landslides from Massive Rock Slope Failure*. NATO Science Series IV, Earth and Environmental Sciences v. 49. Springer, Dordrecht, pp. 285–304.

16. McSaveney, M.J., Davies, T.R.H. and Hodgson, K.A. (2000) A contrast in deposit style and process between large and small rock avalanches, in E. Bromhead, N. Dixon and M.-L. Ibsen (eds.), *Landslides in Research, Theory and Practice*. Thomas Telford Publishing, London, 1053–1058.

17. McSaveney, M.J. and Downes, G. (2002) Application of landslide seismology to some New Zealand rock avalanches, in J. Rybar, J. Stemberk and P. Wagner (eds.), *Landslides*. Balkema, Lisse, pp. 649–654.

18. Nash, T. (2004) Engineering geological assessment of selected landslide dams formed from the 1929 Murchison and 1968 Inangahua earthquakes, Unpublished M.Sc. (Eng Geol) thesis, University of Canterbury, 230p.

19. Nedderman, R. (1992) *Statics and Kinematics of Granular Materials*. Cambridge University Press, Cambridge.

20. Reyners, M., McGinty, P., Cox, S., Turnbull, I., O'Neill, T., Gledhill, K., Hancox, G., Beavan, J., Matheson, D., McVerry, G., Cousins, J., Zhao, J., Cowan, H., Caldwell, G. and Bennie, S. the GeoNet team (2003) The Mw7.2 Fiordland earthquake of August 21, 2003: Background and preliminary results, *Bulletin of the New Zealand Society for Earthquake Engineering* **36**, 233–248.

21. Sammis, C., King, G. and Biegel, R. (1987) The kinematics of gouge formation, *Pure and Applied Geophysics* **125**, 777–812.

22. Scherbakov, R. and Turcotte, D.L. (2004) Damage and self-similarity in fracture, *Theoretical and Applied Fracture Mechanics* **39**, 245–258.

23. Scherbakov, R. and Turcotte, D.L. (2004) A damage mechanics model for aftershocks, *Pure and Applied Geophysics* **161**, 2379–2391.

24. Stark, C.P. and Hovius, N. (2001) The characterization of landslide size distributions, *Geophysical Research Letters* **28**, 1091–1094.

25. Wawersik, W.R. and Fairhurst, C. (1970) A study of brittle rock fracture in laboratory compression experiments, *International Journal of Rock Mechanics and Mining Sciences* **7**, 561–575.